MATEC Web of Conferences **13**, 04019 (2014)
DOI: 10.1051/matecconf/ 20141304019


# Structural Analysis of Basalt Fiber Reinforced Plastic Wind Turbine Blade

Ali Nawaz Mengal[1, a], Saravanan Karuppanan[1] and Azmi Abdul Wahab[1]

[1]Department of Mechanical Engineering, Universiti Teknologi PETRONAS, 31750 Tronoh, Perak, Malaysia

**Abstract.** In this study, Basalt fiber reinforced plastic (BFRP) wind turbine blade was analyzed and compared with Glass fiber reinforced plastic blade (GFRP). Finite element analysis (FEA) of blade was carried out using ANSYS. Data for FEA was obtained by using rule of mixture. The shell element in ANSYS was used to simulate the wind turbine blade and to conduct its strength analysis. The structural analysis and comparison of blade deformations proved that BFRP wind turbine blade has better strength compared to GFRP wind turbine blade.

## 1 Introduction

With increasing energy demands, competitive prices and growing environmental concerns, wind power system is increasingly receiving the attention of mankind. The blades of wind turbine rotor are the most critical component in wind power system [1]. For increased power generation and a greater efficiency the general trend is for larger wind turbine blades with an increased rotor diameter [2].

According to statistical data provided by World Wind Energy Association, the size of modern wind turbine is 100 times bigger than that of wind turbine in 1980s and the blade length is more than 80 meters [3]. With the increase in the size of wind turbine blades the material selection has become crucial focusing many factors such as stiffness, fatigue strength, breaking toughness, rigidity, less weight, low cost and potential of recycling [4] . In order to improve the design, strength and fatigue life of wind turbine blades, it is necessary to investigate new composite materials.

Basalt reinforced composites are recently developed materials. Basalt fibers with their excellent mechanical properties represent an interesting alternative composite material for modern wind turbine blades [4, 5]. In this study BFRP and GFRP wind turbine blades were analyzed and compared.

## 2 Blade structure

In this study the blade completed in solid works was imported to ANSYS. The blade was partitioned into five segments. This enables the application of different loads at different sections of the blade.

[a] Corresponding author : aliract@gmail.com



Article available at http://www.matec-conferences.org or http://dx.doi.org/10.1051/matecconf/20141304019

The length of the blade is 41.25 meter so the length of each segment is 8.25 meter. The blade was composed of an outer surface and an inner spar. For the skin, hexahedral shell element (SHELL 181) with four nodes was considered. Hexahedral shell elements are more efficient than tetrahedral elements and well suited for linear, large rotation and large strain nonlinear application [6]. The skin thickness of the blade is 10 mm and the spar thickness is 50 mm.

## 3 Material properties

Blades currently used for large wind turbines are composed of fiber composite materials so that a stiff, lightweight design with a high fatigue life is achieved. The fibers for wind turbine blades are typically oriented to $0^o$, $+45^o$, and $-45^o$ orientations, with $0^o$ being parallel to the blade span direction [2].

In this study, basalt fiber/epoxy and glass fiber/epoxy was considered as the material of the blade. Different commercial products which are made by basalt fiber proved that this material can be an interesting alternative composite fiber for wind turbine rotor blades [7]. Compared to glass fiber, most references claimed that basalt fiber has higher modulus and strength [8]. Material properties were calculated according to rule of mixture for composite materials [9]. Element lay up for the blade is taken as (0/0/+45,-45/0/0).

The material properties of a layup were determined by making some assumptions regarding the behavior of its constituents. The primary assumption is that the fiber is the main load bearing member and strong constituent of a composite lamina, and the matrix is weak constituent of a composite lamina whose main function is to protect the fibers from severe environmental effects. In this analysis, an orthotropic composite lamina is considered to derive expressions for the modulus of elasticity. First, the procedure for determining the elastic modulus $E_c$ is described. The corresponding stresses in the fiber and the matrix are given by

$$\sigma_f = E_f \varepsilon_1;\ \sigma_m = E_m \varepsilon_1 \tag{1}$$

Where $E_f$ and $E_m$ are the elastic modulus of the fiber and the matrix, respectively. The cross-sectional area $A$ is made up of the area of the fiber $A_f$ and the area of the matrix $A_m$. If the total stress acting on the cross-section is $\sigma_1$, then the total load acting on the cross-section is

$$P = \sigma_1 A = E_c \varepsilon_1 A = \sigma_f A_f + \sigma_m A_m \tag{2}$$

From the above equation, the elastic moduli in the 1-direction can be written as

$$E_c = E_f (A_f / A) + E_m (A_m / A) \tag{3}$$

The volume fraction of the fiber $V_f$ and the matrix $V_m$ can be expressed in terms of areas of the fiber and the matrix as

$$V_f = A_f / A;\ V_m = A_m / A \tag{4}$$

Substituting Equation (4) in Equation (3), we can write the modulus in the 1-direction as

$$E_c = E_f V_f + E_m V_m \tag{5}$$

Equation (5) is the well-known rule of mixtures for obtaining the equivalent modulus of the ply in the direction of the fibers. Now to factor the rule of mixture formula according to fiber angle we will use efficiency factor (Krenchel factor) in equation 3.5, giving

$$\eta_\theta = \sum a_n \cos^4 \theta \tag{6}$$

$$E_c = \eta_\theta E_f V_f + E_m V_m \tag{7}$$

The major Poisson's ratio $\nu_{12}$ is determined as follows

$$v_{12} = v_f V_f + v_m (1-V_f) \quad (8)$$

By adopting a similar procedure the shear modulus in terms of the constituent properties can be written as

$$1/G_{12} = V_f / G_f + (1-V_f) / G_m \quad (9)$$

In Table 1 the structural mechanical properties are listed. They have been extracted from the respective data sheet [10]. By using the values of Table 1 in equation 7, 8, and 9, the orthotropic mechanical properties of BFRP and GFRP were obtained. In Table 2 mechanical properties of BFRP and GFRP are listed.

**Table 1.** Structural mechanical properties of the basalt fibers, glass fiber and the epoxy.

| | Basalt | Glass | Epoxy |
|---|---|---|---|
| Density, $\rho$, g/cm$^3$ | 2.7 | 2.6 | 1.15 |
| Elastic Modulus, $E$, (GPa) | 89 | 72.4 | 2.65 |
| Shear modulus, $G$, (GPa) | 21.7 | 26 | 0.98 |
| Poisson's ratio, $v$ | 0.2 | 0.22 | 0.35 |

**Table 2.** Mechanical properties of BFRP and GFRP

| | Basalt fiber (MPa) | Glass fiber (MPa) |
|---|---|---|
| $E_x$ | 37700 | 29700 |
| $E_y$ | 5237 | 4000 |
| $E_z$ | 5237 | 4000 |
| $v_{xy}$ | 0.2 | 0.22 |
| $v_{yz}$ | 0.21 | 0.23 |
| $v_{xz}$ | 0.21 | 0.23 |
| $G_{xy}$ | 2050 | 2070 |
| $G_{yz}$ | 3630 | 3070 |
| $G_{xz}$ | 3630 | 3070 |

## 4 Finite element analysis

For numerical analysis of blade, ANSYS workbench finite element software was used. The composite material used for both the skin and spar of wind turbine blade is the same. The skin was meshed with hexahedral shell element (SHELL 181). A skin thickness of 10 mm and a spar thickness of 50 mm were chosen. The thickness of blade root is 40 mm, and the thickness of blade tip is 20 mm. The thickness of blade sequentially reduces from root to tip. The finite element model of the blade and its partial enlarged view is shown in Figure 1 and 2. Figure 2 shows an optimum mesh in which the element size for all five parts of the body was set to 0.2 m. The number of elements was 7709, and the number of nodes was 7502. Linear orthotropic material model was used to define the skin properties (defined by elastic modulus $E$, Poisson's ratio $\upsilon$ and shear modulus $G$). The skin lay-up was depicted

as single layer to simplify the model and to reduce calculation time. Material properties were calculated according to the rule of mixture, which gave a convenient and rapid evaluation of stiffness characteristics.

For the simulation, the root section of the blade was fixed, and the force was applied at the tip end of the blade. The standard gravitation force was also considered in this analysis. Figure 3 shows the principle scheme of the structure strength and stiffness analysis. In Figure 3 the fixed support of the root was at *A*. Acting force (3000 N) was applied at *B*, measured 39 m from the free end of the root, and standard earth gravity (9.806 m/s$^2$) was applied at *C*.

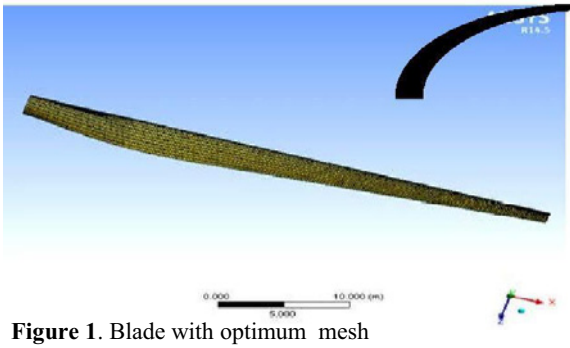

**Figure 1**. Blade with optimum mesh

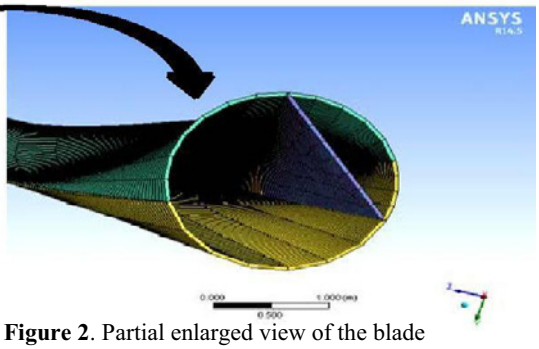

**Figure 2**. Partial enlarged view of the blade

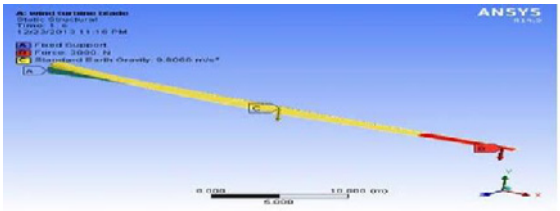

**Figure 3**.Results of structural analysis

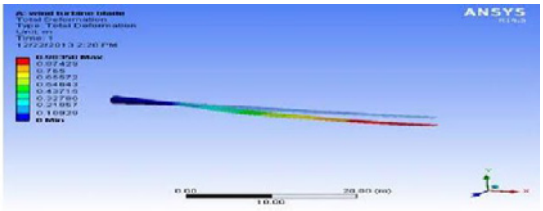

**Figure 4**. GFRP blade deformation

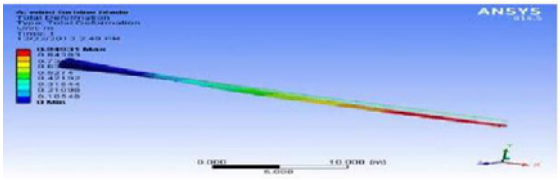

**Figure 5**. BFRP Blade deformation

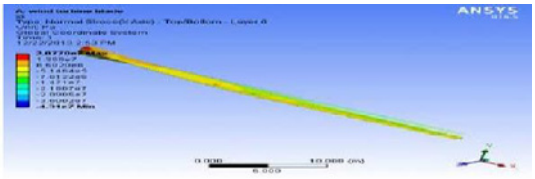

**Figure 6**. Normal stress for GFRP

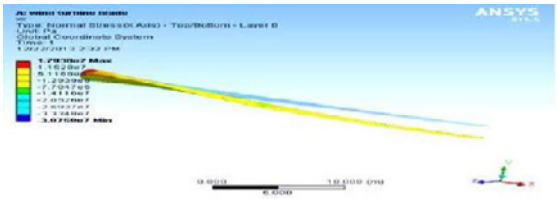

**Figure 7**. Normal stress for BFRP

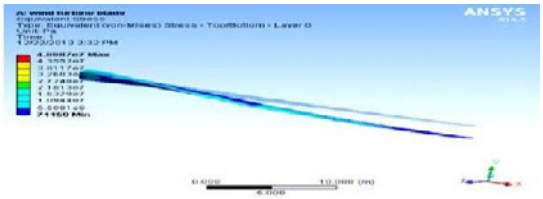

**Figure 8**. Von Mises equivalent stresses of BFRP

## 5 Results and discussion

From the obtained FEA results it can be seen that the maximum deformation of the blade was at the tip. The minimum deformation was at the blade root where hardly any deformation emerges, because fully constrained conditions were applied at the root, to meet the requirements of stability. Figure 4 and 5 show the maximum displacement in GFRP and BFRP. The values of maximum deformation

were 0.98358 m and 0.94931 m for GFRP and BFRP, respectively.

Figure 6 and 7 show the ANSYS normal stress results for GFRP and BFRP wind turbine blades, respectively. It can be seen that stress concentration occurred at the blade root in both cases. This concentration was due to the contact between beginning of the spar and blade and can be neglected. Throughout remainder of the blade the stress was far below the maximum skin stress, and the deformation was within limits. The normal stress values for GFRP and BFRP were 2.0778 MPa and 1.7938 MPa, respectively.

Figure 8 shows the ANSYS results for von Mises equivalent stress. According to the results of this analysis, the maximum stress in the blade occurs at the origination point of spar. The maximum equivalent stress values for GFRP and BFRP were 510 MPa and 489 MPa, respectively.

## 6 Conclusion

Structural analysis of BFRP and GFRP wind turbine blade has been performed. FEA model results achieved using ANSYS have confirmed the better strength and stiffness of BFRP wind turbine blade. This analysis showed that the deflection and stress developed in BFRP blades were less as compared to GFRP blade in same force condition, thickness and boundary condition. From this analysis it can be concluded that

(i) Basalt fiber has better strength and stiffness than glass fiber.
(ii) Basalt fiber for their wide range of good mechanical properties offers an interesting economic alternative for modern wind turbine blades.

However prior to the implementation of basalt fiber as the new composite material for wind turbine blades, experimental investigation is needed, especially when dealing with their fatigue behavior in order to utilize the benefits associated with the material.

## References

[1] L. Mishnaevsky, Composite materials in wind energy technology, Encyclopedia of Life Support System (EOLSS); pp. 11- 42 (2010)

[2] O.T. Thomson, Sandwich materials for wind turbine blades: Present and Future, J. Sandw Struct. Mater (2009)

[3] L. Feng, China Wind Power Report Beijing: China Environmental Science Press; pp. 40-43 (2012)

[4] A.N. Mengal, S. Karuppanan, A.A. Wahab, Basalt carbon hybrid composite for wind turbine rotor blade: A short review, AMR. (to be published)

[5] B. Mislavsk, Advanced basalt fiber in high-tech applications, JEC Magazine. **44,** 22-24 (2008)

[6] O. Pabut, G. Alikas, Modal validation and structure analysis of small wind turbine blade, 8th International Baltic Conference (2012)

[7] Information on http: //www.basfiber.com /application

[8] C.J. Burgoyne, N. Taranu, K. Pilakoutas, A. Serbescu, V. Tamuzs, A. Weber, FRP reinforcement in RC structures, FIB technical report. Stuttgart: Sprint Digital Druck Editor (2007)

[9] B.D. Agarwal, L.J. Broutman, *Analysis and performance of fiber composites*, 2nd Edition, Wiley, New York, p.61 (1990)

[10] N. Tranu, R. Hohan, L. Bejan, Longitudinal Stiffness Characteristics of Unidirectional Fiber Reinforced Polymeric Composites Subjected To Tension, Tomul LVIII (LXII), (2012)